Trends of exchange interactions in dilute magnetic semiconductors

2007 J. Phys.: Condens. Matter 19 436227

(http://iopscience.iop.org/0953-8984/19/43/436227)

IOP PUBLISHING JOURNAL OF PHYSICS: CONDENSED MATTER

J. Phys.: Condens. Matter **19** (2007) 436227 (12pp) doi:10.1088/0953-8984/19/43/436227

Trends of exchange interactions in dilute magnetic semiconductors

B Belhadji[1], L Bergqvist[1], R Zeller[1], P H Dederichs[1], K Sato[2] and H Katayama-Yoshida[2]

[1] Institut fuer Festkoerperforschung, Forschungszentrum Juelich, D-52425 Juelich, Germany
[2] Institute for Scientific and Industrial Research, Osaka University, 8-1 Mihogaoka, Ibaraki, Osaka 567-0047, Japan

E-mail: p.h.dederichs@fz-juelich.de

Received 6 September 2007
Published 9 October 2007
Online at stacks.iop.org/JPhysCM/19/436227

Abstract

We discuss the importance of different exchange mechanisms like double exchange, p–d exchange and anti-ferromagnetic as well as ferromagnetic superexchange in dilute magnetic semiconductors (DMSs). Based on the coherent potential approximation for the electronic structure of the DMSs we show that the different mechanisms exhibit different dependences on the concentration of the magnetic impurities, on the hybridization with the wavefunctions of neighbouring impurities and on the position of the Fermi level in the band gap. However, common to all mechanisms is that, as long as half-metallicity is preserved, they are determined by the hybridization with the orbitals of neighbouring impurities and of the resulting energy gain due to the formation of bonding and anti-bonding hybrids. By calculating the exchange coupling constants $J_{ij}(E_F)$ as a function of the position of the Fermi level we obtain a universal trend for the exchange interactions with band filling.

(Some figures in this article are in colour only in the electronic version)

1. Introduction

Dilute magnetic semiconductors (DMSs) like (Ga, Mn)As, (Ga, Mn)N or (Zn, Cr)Te are regarded as promising materials for spintronics [1–4]. They show a particularly rich magnetic behaviour, being governed by different kinds of exchange interactions like Zener's double exchange [5–8], Zener's p–d exchange [9–13] and superexchange [14, 15]. While the magnetic properties can be successfully calculated by *ab initio* methods and many calculations for such systems have been performed (see e.g. [3, 16–18]), the physical understanding of the exchange mechanisms involved is a very delicate and difficult problem, since no simple and elementary magnetic interaction exists, such that a multitude of mechanisms can lead to ferromagnetism or anti-ferromagnetism and some of them might even act simultaneously.

The discussions in the present paper are based on two approximations. Firstly we assume that the magnetic moments of the transition metal impurities like Mn in GaAs are very stable and do not change much by rotation and the interactions with neighbouring impurities. *Ab initio* calculations show that this assumption is well satisfied. This allows us to apply the frozen potential approximation or the 'magnetic force theorem', according to which the total energy is well approximated by the single particle energies. Thus we can concentrate our discussion on the spin-polarized density of states (DOS) only and discuss the interaction effects in the DOS introduced by the hybridization of the wavefunctions with those of neighbouring atoms. Secondly we discuss only the disorder averaged density of states, as obtained by the coherent potential approximation, which provides a mean field description of the electronic structure.

In a previous paper [12] we have discussed the role of double exchange and p–d exchange as the stabilizing mechanisms of ferromagnetism in DMS. We could show that these mechanisms exhibit a very different concentration dependence. Moreover, we showed that in (Ga, Mn)As double exchange prevails in an LDA description of the electronic structure, but p–d exchange in the LDA + U (with $U = 4$ eV). Here we extend this work and discuss the superexchange mechanism in detail. Typical for this mechanism is that it also occurs in insulators and does not require carriers as double and p–d exchange do. We will show that the strength of the superexchange depends strongly on U and that the exchange coupling constants J_{ij} are independent of the concentration. Moreover, superexchange can not only lead to anti-ferromagnetism, but can also promote ferromagnetism, e.g. in (Ga, V)As.

In the last section of this paper we present systematic calculations of the exchange coupling constant $J_{01}(E_F)$ between nearest neighbours for several DMS systems. By artificially changing the Fermi level E_F across the gap region we find a systematic change of the exchange coupling and of the sequence of exchange mechanisms with band filling which is the same for all compound DMSs with zincblende structure. We also expect the same behaviour for DMSs with wurtzite structure, since the additional level splittings induced by the lower symmetry are for typical concentrations smaller than the band broadening.

The *ab initio* calculations have been performed by the Korringa–Kohn–Rostoker coherent potential approximation (KKR–CPA) Green's function method [19, 20]. The exchange coupling constants J_{ij} have been evaluated by the formula given by Liechtenstein [21]

$$J_{ij} = \frac{1}{4\pi} \operatorname{Im} \int^{E_F} \mathrm{d}E \operatorname{Tr} \{(t_i^+ - t_i^-) G_{ij}^+(E) (t_j^+ - t_j^-) G_{ji}^-(E)\}, \tag{1}$$

where $G_{ij}^{\pm}(E)$ are the KKR Green's functions for spin direction + or − connecting the sites i and j and t_i are the site dependent scattering matrices. To average over the disorder, the Green's functions are replaced by the CPA Green's functions [21].

2. Summary of double exchange and p–d exchange mechanisms

In this chapter we give a short summary of Zener's double exchange mechanism [8] in DMSs as well as Zener's kinetic p–d exchange mechanism [10–13]. We discuss here only the qualitative trends, since they are important for the discussion of the superexchange in the next sections. A more detailed description of both mechanisms has been published in [12].

2.1. Double exchange

Figure 1(a) shows schematically the spin-polarized density of states (DOS) of a transition metal impurity in a wide band gap semiconductor, such as for Mn or Cr in GaN. The Fermi level E_F is assumed to fall within the partially occupied majority band of the t_{2g} impurity state. The stabilization of the ferromagnetic state arises from the width of the impurity band. For

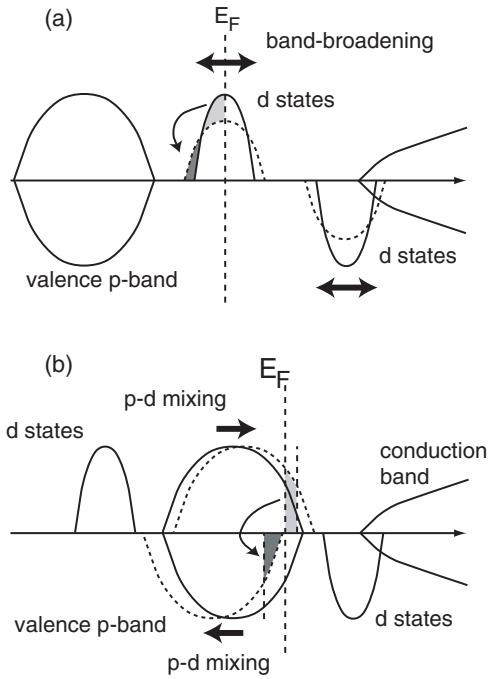

Figure 1. (a) Schematic diagram of the spin-polarized DOS of a transition metal impurity in a wide gap semiconductor. (b) Schematic diagram of the spin-polarized DOS in the case of p–d exchange, when the majority d level lies below the valence p band and the minority level above.

instance, if the Fermi level lies in the middle of the impurity band, as is assumed in the figure, only bonding states are occupied, while the anti-bonding states are empty. Now it is important to realize that the band width of the impurity band scales as the square root $\sqrt{c}$ of the impurity concentration c and varies linear with the hopping matrix element t between neighbouring impurities. This is the double exchange mechanism, leading to an energy gain of the ferromagnetic state proportional to

$$\Delta E_{\mathrm{DX}} \sim \sqrt{c}|t|. \tag{2}$$

A detailed derivation has been given in [12]. This behaviour is basically well known for e.g. transition metals, the band width of which scales as the square root $\sqrt{N_{\mathrm{c}}}$ of the coordination number N_{c}.

Due to the disorder in DMS the effective coordination number is proportional to c. The double exchange mechanism is very strong. Thus, when the Fermi level lies within the impurity band, usually double exchange wins (e.g. over anti-ferromagnetic superexchange) and stabilizes the ferromagnetic configuration. Moreover, since in wide gap semiconductors the deep impurity level wavefunctions as well as the host Green functions are well localized, this kind of double exchange interaction is very short ranged, which has the important consequence that in the dilute limit the ferromagnetism cannot percolate through the crystal and the Curie temperatures are very small [22–24].

2.2. Kinetic p–d exchange

Figure 1(b) sketches the physical situation for Zener's p–d exchange [9, 11–13]. In narrow gap semiconductors like GaSb or InSb the Mn d majority level lies below or at the lower edge of

the Sb p band, while the minority d level lies well above E_F. This means that Mn has a moment of 5 μ_B, well localized at the Mn site. Then, in the neutral state, due to charge neutrality one electron per Mn atom is missing in the valence band as indicated by the position of E_F in figure 1(b). Since the impurity d wavefunctions hybridize with the p wavefunctions of the neighbouring p elements, the majority p band is shifted to higher energies, while the minority p band is shifted to lower energies due to hybridization with the higher lying minority d state (figure 1(b)) [11]. If the hybridization is sufficiently strong, the minority p band becomes completely occupied, while one electron per Mn atom is missing in the majority p band, leading to a half-metallic density of states. As a result the Sb atoms carry small moments of 1 μ_B/Mn in total, being aligned anti-parallel to the local moment of Mn, such that the total moment per Mn atom is 4 μ_B. Usually the spin polarization of the host is described by a Kondo model Hamiltonian without explicitly introducing the Mn atoms. We refer to the literature on this [2, 10]. The physical reason is, however, the p–d hybridization with the impurity d states [11–13]. The host spin polarization of a second or third impurity wants to align parallel to the one of the first impurity, leading effectively to a ferromagnetic coupling of the Mn atoms. A more detailed discussion of this interaction is given by Dalpian *et al* [13]. Most important is that this p–d exchange coupling is relatively weak, but long ranged. In the mean field approximation the Curie temperature T_C^{MFA}, given by two-thirds of the energy difference between the ferromagnetic and the disordered local moment (DLM) states, scales linearly with the concentration c, while in the case of double exchange T_C^{MFA} varies as $T_C^{MFA} \sim \sqrt{c}$.

Double exchange and p–d exchange are extreme cases of a more general type of interaction, where both mechanisms can occur simultaneously. For instance, realistic calculations show that in (Ga, Mn)N the d level is deep in the gap and the behaviour is dominated by double exchange, while (Ga, Mn)Sb is dominated by p–d exchange [12]. In contrast to this (Ga, Mn)As and (Ga, Mn)P are intermediate cases. LDA calculations yield for (Ga, Mn)As both a $\sqrt{c}$-behaviour typical for double exchange and an indication of a linear behaviour for larger concentrations. In LDA + U calculations the Mn d level is shifted to lower energies and a more linear concentration dependence is obtained for T_C^{MFA}, showing that the p–d exchange becomes more important, in qualitative agreement with the above discussion.

Characteristic for both interactions is that the Fermi level lies within the band. If, in the case of p–d exchange, the Fermi level lies above the valence band or, in the case of double exchange, above or below the impurity d band, the hybridization effects are the same, but no energy can be gained to favour ferromagnetism.

3. Superexchange mechanism

Superexchange is different from this, since it does not require a finite density of states at E_F, i.e. it can also occur in an insulator. The reason for this is that it is related to the hybridization of such states which are energetically localized well below *and* well above E_F. Note that superexchange is usually explained by magnetic coupling transferred by ligands, i.e. the p orbitals of the anions. In DMSs the situation is considerably simplified, if we take the impurity gap states as elementary units, which hybridize with each other and transfer the coupling. Of course, these states themselves are hybrids between impurity d states and anion p states, but for the coupling this is of secondary importance.

As an illustrative example figure 2(a) shows the density of states for two impurity systems with moments $\mathbf{S}_1$ and $\mathbf{S}_2$, being anti-parallel aligned and having equal concentrations $c/2$. Since the electronic states with the same spin direction hybridize with each other, the lower occupied energy peaks are shifted to lower energies, the higher empty ones to higher energies. Due to the down-shift of the lower occupied level binding energy is gained, which stabilizes the anti-ferromagnetic coupling.

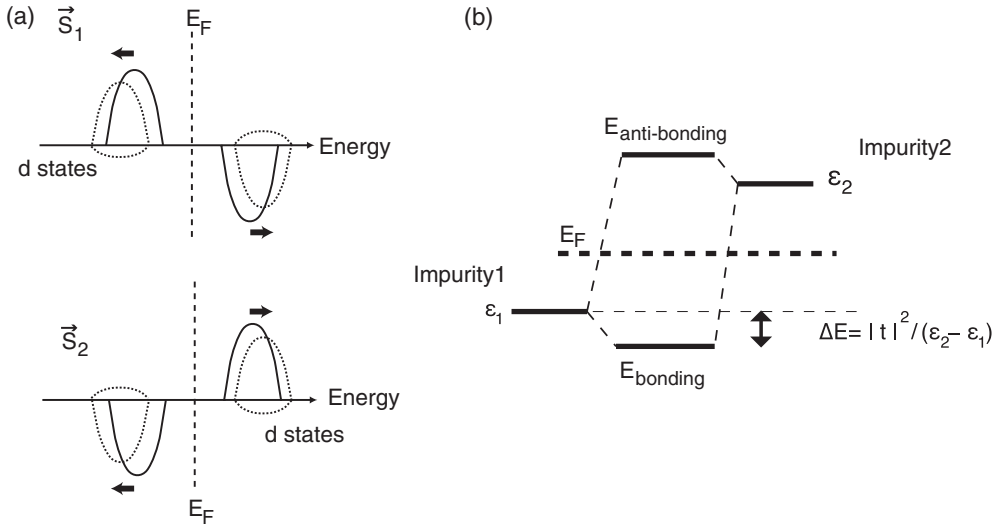

Figure 2. (a) Schematic diagram of the DOS of two anti-parallel aligned impurity systems 1 and 2 with equal concentrations $c/2$. (b) Schematic representation of the hybridization induced energy gain ΔE of equation (4) for a diatomic system with unperturbed levels $\epsilon_1 < \epsilon_2$.

The basic mechanism can be understood from a molecular model with two atomic states with different energies $\epsilon_1 < \epsilon_2$ and a hopping matrix element t; this situation is sketched in figure 2(b). Due to hybridization the molecular levels are given by

$$\epsilon_\pm = \tfrac{1}{2}(\epsilon_1 + \epsilon_2) \pm \sqrt{\left(\tfrac{1}{2}(\epsilon_1 - \epsilon_2)\right)^2 + |t|^2}. \tag{3}$$

If only the lower level ϵ_1 is occupied and moreover $|t| \ll \frac{1}{2}(\epsilon_1 - \epsilon_2)$ the binding energy is given by

$$\Delta E \cong \frac{|t|^2}{\epsilon_2 - \epsilon_1}. \tag{4}$$

When applied to the above two impurity systems with opposite moments and concentrations $c/2$ the energy gain per Mn atom for anti-ferromagnetic coupling is given by

$$\Delta E_{SX} \cong c\frac{|t|^2}{\epsilon^{\uparrow}_{t_{2g}} - \epsilon^{\downarrow}_{t_{2g}}}, \tag{5}$$

where t refers to the hopping element between the impurity t_{2g} states on neighbouring sites and the denominator gives the splitting between the majority and minority t_{2g} levels. The linear c-factor arises from the fact that the effects of several impurities, coupling antiferromagnetically to the aligned one, superimpose on each other. Since there are $c/2$ such impurities, and since the energy is gained in both spin directions, a prefactor c appears.

The superexchange interaction is independent of the position of the Fermi level, as long as this lies between the two impurity bands in figure 2(a). If it enters these bands, e.g. the lower one, it decreases, roughly by a factor of two, if the Fermi level lies in the middle of the band and it vanishes if E_F lies below this band. Thus, if the Fermi level lies in the band, there is a competition between double exchange and superexchange, which is usually won by double exchange, resulting in ferromagnetism, except when E_F approaches the upper band edge, where superexchange takes over, destroying the ferromagnetism. Examples for

magnetically disordered DMSs due to superexchange are Mn in II–VI compounds like ZnSe or CdTe and Fe in III–V compound semiconductors. Moreover (Ga, Mn)As with strong electron doping also belongs to these systems.

Superexchange is a rather strong interaction, since the t_{2g}–t_{2g} overlap is rather large. This is also true for wide gap semiconductors, where the interaction is very short ranged, similar to double exchange. Typical for superexchange is that it strongly depends on the exchange splitting $\epsilon^{\uparrow}_{t_{2g}} - \epsilon^{\downarrow}_{t_{2g}}$. While in LDA this is given by $I \cdot M_{\mathrm{loc}}$, i.e. the exchange integral I times the local moment M_{loc}, in LDA + U this is given by the (usually considerably larger) Hubbard U parameter. Therefore, the LDA can seriously overestimate the superexchange mechanism, as we will demonstrate in section 5 for the case of (Ga, Fe)N.

In the mean field approximation the Curie temperature is given by

$$k_{\mathrm{B}} T_{\mathrm{c}}^{\mathrm{MFA}} = \tfrac{2}{3}\Delta\epsilon, \tag{6}$$

where $\Delta\epsilon$ is the energy difference per Mn impurity between the DLM and the ferromagnetic phases. Due to equation (5) for the superexchange, we expect e.g. for (Ga, Fe)As or (Ga, Fe)N a linear dependence of $T_{\mathrm{C}}^{\mathrm{MFA}}$ on concentration c with a negative slope, which is indeed found in *ab initio* calculations (see figure 3(a)) for (Ga, Fe)N. The negative values can be interpreted as positive Néel temperatures. The calculated exchange coupling constants J_{ij} obtained by using the Liechtenstein formula [21] are plotted in figure 3(b) for the Fe–Fe interactions in (Ga, Fe)N with a concentration of 5%. One observes that basically the interaction is restricted to the nearest neighbours, and that, moreover, the interaction is to a good approximation independent of concentration, which is very different from the case of double or p–d exchange. This can be understood from equation (6). Since $\Delta\epsilon$ is linear in c and on the other hand given by $cJ_0 = c\sum_{j\neq 0} J_{0j} \cong 12cJ_{01}$,where J_{01} is the nearest neighbour coupling constant in the fcc Ga sublattice of zb-GaN, the coupling constant J_{01} should be independent of concentration. Physically, the decisive occupied majority $t^{\uparrow}_{2g}$ band is broadened by concentration, which, however, does not affect the energy gain, since the state is fully occupied. For the same reason in calculations for disordered systems, where we do not make the CPA approximation, we find a much weaker dependence of the nn coupling J_{01} on disorder effects than in double exchange systems [25].

4. Ferromagnetic superexchange

Superexchange can also favour ferromagnetism. For this we consider the case where the Fermi level falls between the majority $e^{\uparrow}_{g}$ state and the majority $t^{\uparrow}_{2g}$ state, which is the case for (Ga, V)As or, in the case of minority states, for (Zn, Co)O. The first case is illustrated in figure 4. Here the orbitals of the occupied majority $e^{\uparrow}_{g}$ level of impurity 1 hybridize with empty majority $t^{\uparrow}_{2g}$ orbitals of the neighbouring impurity 2 and vice versa. As a result, the occupied $e^{\uparrow}_{g}$ orbitals are slightly shifted to lower energies, in this way stabilizing ferromagnetism by superexchange. Quite analogous to the previous result (4), for ferromagnetic superexchange the energy gain is given by

$$\Delta E_{\mathrm{SX}} = 2c\frac{|t|^2}{\epsilon^{\uparrow}_{t_{2g}} - \epsilon^{\uparrow}_{e_g}}, \tag{7}$$

where t is the hopping matrix element between the $e^{\uparrow}_{g}$ state and the $t^{\uparrow}_{2g}$ state on the neighbouring impurity, which is expected to be considerably smaller than the t_{2g}–t_{2g} hopping, since the e_g orbitals are very localized. (For the same reason, double exchange resulting from the broadening of the e_g band, i.e. the e_g–e_g hopping, is very weak and practically negligible.) However, the smallness of the e_g–t_{2g} hopping element is partially balanced by

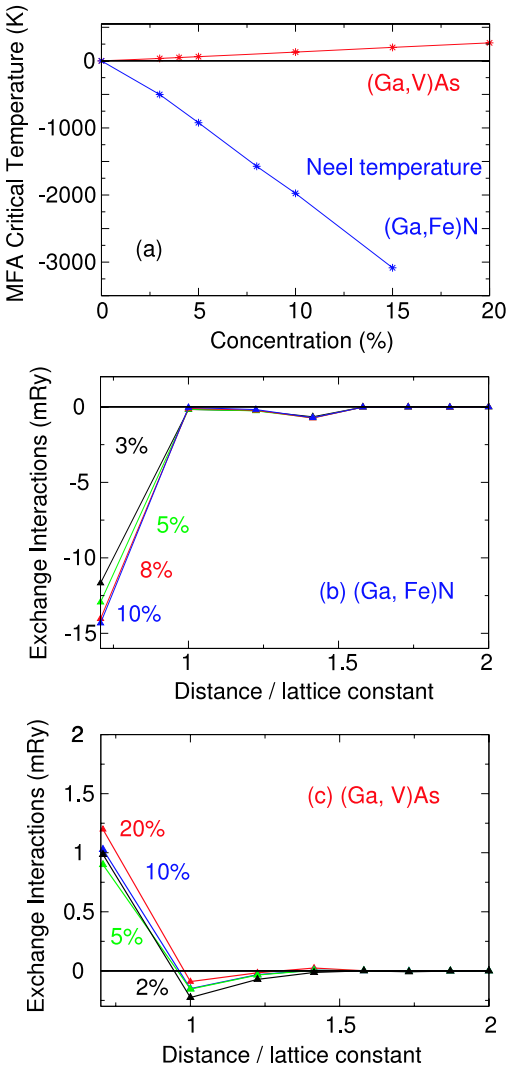

Figure 3. (a) Mean field Curie temperatures T_C^{MFA} for (Ga, Fe)N and (Ga, V)As as a function of impurity concentration c. (b) Exchange coupling constants J_{ij} for the Fe–Fe coupling in (Ga, Fe)N for various concentrations as a function of the distance. (c) Exchange coupling constants J_{ij} for the V–V interaction in (Ga, V)As.

the denominator $\epsilon^{\uparrow}_{t_{2g}} - \epsilon^{\uparrow}_{eg}$, representing the relatively small crystal field splitting. For the case of (Ga, V)As the mean field Curie temperatures are given in figure 3(a), demonstrating that in DMS the ferromagnetic superexchange is considerably smaller than the anti-ferromagnetic superexchange relevant for (Ga, Fe)N. The ferromagnetic coupling constants relevant for the V–V interaction in (Ga, V)As are shown in figure 3(c). The interactions are rather weak and short ranged. For the same reason as the Fe–Fe interactions in (Ga, Fe)N they depend only slightly on the concentration. Another analogy to the anti-ferromagnetic superexchange is the strong dependence on Hubbard U effects. Since the occupied states are pushed to lower energies and unoccupied states to higher energies, the crystal field splitting will increase and the ferromagnetic superexchange will decrease even further.

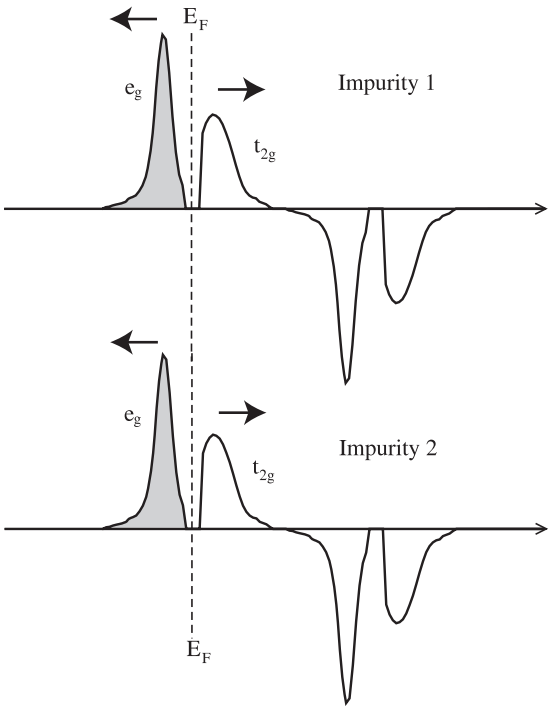

Figure 4. Schematic diagram of the spin-polarized DOS of two V impurities in ferromagnetic (Ga, V)As.

5. Universal behaviour of exchange interactions in DMSs

In the past selfconsistent *ab initio* calculations of the exchange coupling constants have been performed for a large number of DMSs by using the LMTO–CPA or KKR–CPA method in connection with the Liechtenstein formula (equation (1)) for the coupling constants [22, 23, 18, 24, 26]. Our calculations show, however, that the trends of the exchange interactions can be seen more clearly if in equation (1) the integrand is evaluated selfconsistently, while the Fermi level is varied artificially over the band gap region.

To some extent, this is a good approximation for the electronic structure for doped materials. Unfortunately, this approximation cannot be justified by the magnetic force theorem, since the charge is varied by the change of E_F. On the other hand the topology of the impurity states, i.e. the sequence e_g below t_{2g} and majority states below minority states is always the same, and basically determines the exchange mechanisms, and therefore this approximation makes sense. This is also shown by the similarity of the results obtained on the basis of selfconsistent calculations for different DMS systems. Figures 5(a)–(c) show the results obtained in this way for (a) (Ga, Mn)N, (b) (Ga, Mn)As and (c) (Ga, Fe)N. While these results are based on LDA calculations, figure 5(d) shows in addition the (Ga, Fe)N results as obtained by the LDA + U with $U = 4$ eV. In all cases an impurity concentration of 5% is assumed. The dashed (red) line shows the local density of states (DOS) of the impurity, while the full (blue) line denotes the exchange integral $J_{01}(E_F^*)$ for the first nearest neighbour as a function of the artificially varied Fermi level E_F^*. Firstly we see that the structures of the impurity bands are in all cases very similar and that the same is also true for the $J_{01}(E_F^*)$

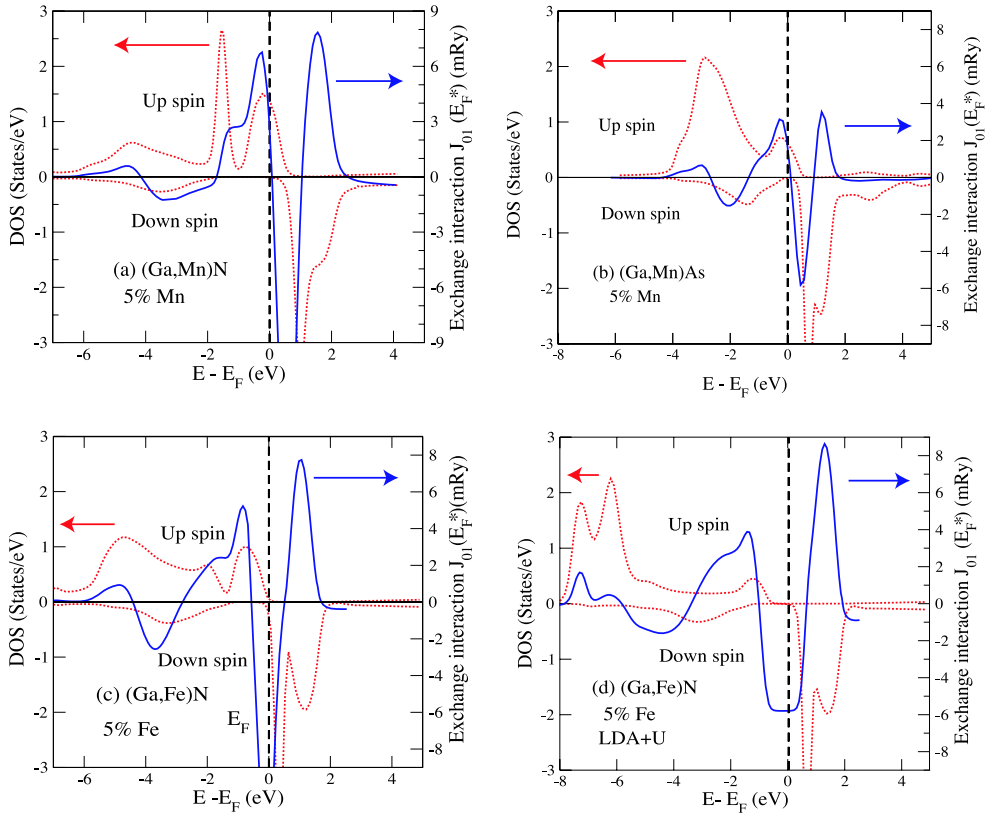

Figure 5. Spin-polarized local DOS of an impurity in DMS (dashed (red) curves, left scale) as a function of E–E_F. Exchange coupling constant $J_{01}(E_F^*)$ for nearest neighbour impurities (full (blue) curve, right scale) as a function of an arbitrary change of E_F^*. (a) 5% Mn in (Ga, Mn)N, (b) 5% Mn in (Ga, Mn)As, (c) 5% Fe in (Ga, Fe)N (LDA method), (d) 5% Fe in (Ga, Fe)N (LDA + U with $U = 4$ eV).

curves, which basically follow the DOS structures. Of course, we should expect this from the previous discussions, since e.g. double exchange should dominate in the t_{2g} bands, while antiferromagnetic superexchange should prevail between the majority and the minority t_{2g} states.

Starting with (Ga, Mn)N we obtain a small positive (ferromagnetic) contribution from the bottom of the valence p band and small negative values in the upper part of the band. At the bottom of the conduction band we have small negative values. However, these values are small compared to the values from the impurity bands. Within the lowest of these, the majority $e_g^\uparrow$ band, the exchange interaction is ferromagnetic and strongly increases to a maximum at the upper edge of this impurity band and a plateau value between the $e_g^\uparrow$ and $t_{2g}^\uparrow$ states. These interactions are due to ferromagnetic superexchange, arising from the hybridization of the $e_g^\uparrow$ states with the $t_{2g}^\uparrow$ states on the neighbouring sites. Within the $t_{2g}^\uparrow$ band we obtain a strong double exchange contribution stabilizing ferromagnetism due to the hybridization induced broadening of the $t_{2g}^\uparrow$ band. However, already in the middle of the $t_{2g}^\uparrow$ band the ferromagnetic exchange coupling decreases again as a result of the strong superexchange resulting from the hybridization of the $t_{2g}^\uparrow$ and $e_g^\downarrow$ states on neighbouring sites. The maximum of the antiferromagnetic coupling occurs between the centres of the $t_{2g}^\uparrow$ and $e_g^\downarrow$ bands.

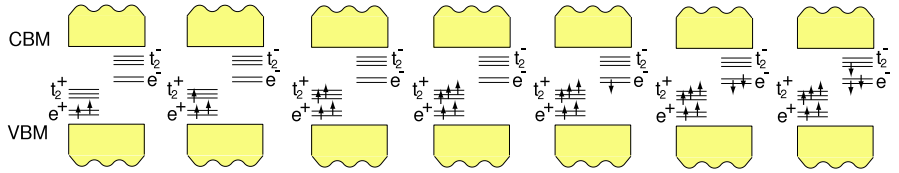

II-VI	$Ti^{2+}(3d^2)$	$V^{2+}(3d^3)$	$Cr^{2+}(3d^4)$	$Mn^{2+}(3d^5)$	$Fe^{2+}(3d^6)$	$Co^{2+}(3d^7)$	$Ni^{2+}(3d^8)$
III-V	$V^{3+}(3d^2)$	$Cr^{3+}(3d^3)$	$Mn^{3+}(3d^4)$	$Fe^{3+}(3d^5)$	$Co^{3+}(3d^6)$	$Ni^{3+}(3d^7)$	$Cu^{3+}(3d^8)$
Double or p-d exchange	—	**FM**	**FM**	—	WFM	—	FM
Super-exchange	**FM**	AF	AF	**AF**	AF	FM/AF	AF

Figure 6. Chemical trend of magnetic interactions in II–VI and III–V DMSs in high spin state. FM, ferromagnetic; WFM, weakly ferromagnetic; AF, anti-ferromagnetic. Where possible, the expected ground states are indicated by bold symbols.

The curve then increases again due to ferromagnetic superexchange between the $e_g^{\downarrow}$ and $t_{2g}^{\downarrow}$ orbitals and becomes positive due to the double exchange of the t_{2g} bands, falling down to small negative values when the t_{2g} band is filled. The trends for Fe in GaN (figure 5(c)) are very much the same. For (Ga, Mn)As we observe an interesting variation arising from the down-shift of the $e_g^{\uparrow}$ and $t_{2g}^{\uparrow}$ levels into the valence band. Below the $t_{2g}^{\uparrow}$ double exchange peak we see a small shoulder, reminiscent of the $e_g^{\uparrow}$–$t_{2g}^{\uparrow}$ ferromagnetic superexchange mechanism. This shoulder is more clearly seen in (Ga, Fe)N, where the $e_g^{\uparrow}$ peak can be still seen in the DOS.

Finally, figure 5(d) shows the resulting DOS curve and the exchange interactions for the case of (Ga, Fe)N calculated in the LDA + U with a U-value of 4 eV. One observes a much larger exchange splitting of the spin-polarized DOS accompanied by a strong reduction of the anti-ferromagnetic superexchange, as discussed in section 4. In fact, the selfconsistent $J_{01}(E_F)$ value for the Fe–Fe nearest neighbours is reduced from -13 to -6 mRyd, a quite remarkable effect.

Thus we see that the exchange interaction curve follows very much the DOS curves and therefore shows a universal behaviour for all wide gap DMSs with zb structure. These universal trends of the exchange interactions are summarized in figure 6. In the figure, the electronic configurations of transition metal impurities in DMSs are shown based on the assumption of high spin states. As a result of the competition between the double (or p–d) exchange and the superexchange interaction, the sign of the total exchange interaction is determined as shown in figure 5. When the trends of the $J_{01}(E_F^*)$ curves are simple and clear, we have indicated in figure 6 the expected ground state (FM or AF) by bold letters. This is easy for the first half of the table in figure 6, when the majority states are filled. For instance, Mn in III–V compounds always couples ferromagnetically either due to p–d exchange, as in (Ga, Mn)As, or due to double exchange, as in (Ga, Mn)N. For the case of Mn in II–VI or Fe in III–V, anti-ferromagnetic superexchange leads to a disordered state. However, the situation is more complicated once the minority states are filled, since several complications arise. Firstly, in LDA the band gap is underestimated and the $e_g^{\downarrow}$ and $t_{2g}^{\downarrow}$ states are often located already in the lower part of the conduction bands. Moreover, the $e_g^{\downarrow}$ and $t_{2g}^{\downarrow}$ impurity bands tend to overlap, so that half-metallicity is lost and the different exchange mechanisms cannot be separated easily. Moreover, LDA and LDA + U calculations can give qualitatively different results,

since in LDA we might have an overlap of the peaks, but in LDA + U a clear separation. Fe in II–VI compounds couples antiferromagnetically in LDA calculation [3]. Co in II–VI compounds is considerably more complicated, since we have in this case a competition between ferromagnetic superexchange, arising from the hybridization of the occupied $e_g^{\downarrow}$ states with the empty $t_{2g}^{\downarrow}$ states, and anti-ferromagnetic superexchange due to the hybridization of the occupied $t_{2g}^{\uparrow}$ states with the empty $t_{2g}^{\downarrow}$ states. In LDA [3] Co in ZnO couples ferromagnetically, but in ZnS, ZnSe and ZnTe it couples antiferromagnetically. Thus realistic calculations for a given material can be difficult and depend on such details as the value of the band gap and the Hubbard U parameter; however, the trends of the exchange interactions are universal and can be explained by the simple description of the exchange interactions presented in sections 2, 3 and 4.

6. Summary

In this paper we have discussed the trends of exchange interactions in dilute magnetic semiconductors (DMSs). Our main emphasis lies on the understanding of the roles of the different exchange mechanisms like double exchange, p–d exchange and superexchange for the magnetic properties of DMSs. Our qualitative discussion is based on the density of states as obtained by the coherent potential approximation, which provides a reliable mean field description of the electronic structure of disordered systems. All exchange mechanisms can be explained by the hybridizations of the impurity state wavefunctions with the wavefunctions of neighbouring impurities and the resulting energy gain due to the formation of bonding and anti-bonding hybrids. Each mechanism has a characteristic dependence on the hybridizing wavefunctions involved, its concentration dependence and the position of the Fermi level. Calculations of the exchange coupling constants $J_{01}(E_F)$ of the nearest neighbours as a function of the Fermi level show a universal behaviour of the exchange interactions with band filling valid for all DMS with zincblende (and wurtzite) structure.

Acknowledgments

This research was partially supported by a Grant-in-Aid for Scientific Research in Priority Areas ‘Quantum simulators and quantum design’ (No 17064014) and ‘Semiconductor nanospintronics’, a Grant-in-Aid for Scientific Research for Young Researchers, JST-CREST, NEDO-nanotech, the 21st Century COE and the JSPS core-to-core programme ‘Computational nano-materials design’. KS acknowledges the financial support from the Kansai Research Foundation for technology promotion (KRF), the Murata Science Foundation and Inoue Foundation for Science (IFS). LB acknowledges support from the European Union (EU) in the framework of Marie Curie Actions for Mobility and Human Resources.

References

[1] Matsukura F, Ohno H and Dietl T 2002 *Handbook of Magnetic Materials* vol 14 (Amsterdam: Elsevier) p 1
[2] Jungwirth T, Sinova J, Mašek J, Kućera J and MacDonald A H 2006 *Rev. Mod. Phys.* **78** 809
[3] Sato K and Katayama-Yoshida H 2002 *Semicond. Sci. Technol.* **17** 367
[4] Dietl T 2002 *Semicond. Sci. Technol.* **17** 377
[5] Zener C 1951 *Phys. Rev.* **82** 403
[6] Anderson P W and Hasegawa H 1955 *Phys. Rev.* **100** 675
[7] de Gennes P G 1960 *Phys. Rev.* **118** 141
[8] Akai H 1998 *Phys. Rev. Lett.* **81** 3002
[9] Zener C 1951 *Phys. Rev.* **81** 440
[10] Dietl T, Ohno H, Matsukura F, Cibert J and Ferrand D 2000 *Science* **287** 1019

[11] Kanamori J and Terakura K 2001 *J. Phys. Soc. Japan* **70** 1433
[12] Sato K, Dederichs P H, Katayama-Yoshida H and Kudrnovský J 2004 *J. Phys.: Condens. Matter* **16** S5491
[13] Dalpian G M, Wei S H, Gong X G, da Silva A J R and Fazzio A 2006 *Solid State Commun.* **138** 353
[14] Kanamori J 1959 *J. Phys. Chem. Solids* **10** 87
[15] Goodenough J B 1955 *Phys. Rev.* **100** 564
[16] Sato K, Dederichs P H and Katayama-Yoshida H 2003 *Europhys. Lett.* **61** 403
[17] Bouzerar G, Kudrnovský J, Bergqvist L and Bruno P 2003 *Phys. Rev.* B **68** 81203(R)
[18] Kudrnovský J, Turek I, Drchal V, Máca F, Weinberger P and Bruno P 2004 *Phys. Rev.* B **69** 115208
[19] Akai H 1989 *J. Phys.: Condens. Matter* **1** 8045
[20] Ebert H and Zeller R 2006 *The SPR-TB-KKR Package* http://olymp.cup.uni-muenchen.de/ak/ebert/SPR-TB-KKR/
[21] Liechtenstein A I, Katsnelson M I, Antropov V P and Gubanov V A 1987 *J. Magn. Magn. Mater.* **67** 65
[22] Bergqvist L, Eriksson O, Kudrnovský J, Drchal V, Korzhavyi P and Turek I 2004 *Phys. Rev. Lett.* **93** 137202
[23] Sato K, Schweika W, Dederichs P H and Katayama-Yoshida H 2004 *Phys. Rev.* B **70** 201202(R)
[24] Fukushima T, Sato K and Katayama-Yoshida H 2004 *Japan. J. Appl. Phys.* **43** L1416
[25] Sato K, Dederichs P H and Katayama-Yoshida H 2007 *ICPS2006: 28th Int. Conf. on the Physics of Semiconductors Proc.* (New York: American Institute of Physics) p 1243
[26] Sato K, Dederichs P H and Katayama-Yoshida H 2007 *J. Phys. Soc. Japan* **76** 024717